SCALING OF EDGE-PLASMA TURBULENCE IN THE CALTECH TOKAMAK

S.J. ZWEBEN, R.W. GOULD
Department of Applied Physics,
California Institute of Technology,
Pasadena, California,
United States of America

ABSTRACT. Edge-plasma turbulence was investigated over a wide range of plasma and field parameters in the Caltech research tokamak. Fluctuation levels and spectra were measured using Langmuir probes in the region r/a = 0.75–1.0. Under almost all conditions the edge plasma was turbulently unstable, with a broad-band fluctuation spectrum in the drift-wave range of frequencies f = 10–1000 kHz. A stable state was observed only in the very cold, low-current discharges formed at unusually high neutral filling pressure. Otherwise, the relative fluctuation level as monitored by the ion saturation current J^+ was very high, in the range $\tilde{J}^+/\bar{J}^+ \cong 0.2–0.8$, while the fluctuation power spectra were roughly invariant in shape. The relative fluctuation level was always highest near the wall and decreased monotonically toward the plasma centre. The same edge turbulence was observed with or without an outer limiter present. The relative fluctuation level was observed to be independent of the local collisionality over a range of nearly 100. The radial variation of $\tilde{J}^+/\bar{J}^+$ can be related to the radial density scale length L_n by $\tilde{J}^+/\bar{J}^+ \cong (3–5)\rho_s/L_n$.

1. INTRODUCTION

Small-scale density fluctuations have often been observed in tokamak experiments using electromagnetic scattering [1–5], Langmuir probes [6–9] or, recently, visible imaging [10, 11]. Generalizing the collective results of these observations, we find at least two common features [12]: (i) the frequency and wavenumber spectra of $\tilde{n}$ are broad, which suggests that the plasma is 'turbulent' on a spatial scale $\lambda \cong \rho_i$ and a frequency scale $f \cong v_*/\rho_i$, where ρ_i is the ion gyroradius and v_* is the electron diamagnetic drift velocity; and (ii) the relative fluctuation levels $\tilde{n}/n$ generally increase from less than 1% at the centre to a maximum of $\tilde{n}/n$ = 5–100% in the edge plasma near the wall [2, 6]. These small-scale 'microscopic' fluctuations have been observed whenever they have been looked for in tokamaks, and they appear to exist independently of the global 'macroscopic' magnetic modes which may be present at the same time.

In view of the probable importance of this turbulence for tokamak particle and energy confinement, extensive theoretical work has been done to examine the low-frequency microstability of the tokamak [13–14]. Recently, several non-linear models have been developed which can simulate the self-interaction of many waves and thus predict broadened wavenumber spectra which are similar to those observed experimentally. However, both the complexity of the theories and the incompleteness of the experimental data base have so far allowed only limited success in fitting such a theory to experiment [15].

In this paper we systematically examine the turbulence of the edge region of the Caltech tokamak. One aim was to search for an operation regime in which the edge plasma would be stable, or at least linearly (non-turbulently) unstable, so that some clue could be obtained as to the physical mechanism normally driving the turbulence. Another aim was to provide a set of data on the 'scaling' of this turbulence in order to test current theoretical models. A third motivation comes from the practical need to understand the sources of cross-field particle diffusion in the edge region in order to optimize the design of limiters or divertors for large tokamak reactors.

The organization of the paper is as follows: Section 2 contains the experimental details about the tokamak and the Langmuir probe techniques, Section 3 describes the experimental results, Section 4 contains a discussion of these results with respect to other experiments and theory, and Section 5 is a summary.

2. EXPERIMENTAL DETAILS

The Caltech research tokamak has the following typical parameters: major radius $R_0 = 45$ cm, minor radius a = 16 cm, toroidal field $B_T = 3.5$ kG, plasma current I = 25 kA, line-averaged density $\bar{n} \cong 10^{12} - 10^{13}$ cm^{-3}, and central electron temperature $T_e \cong 100$ eV (assuming Z = 2). The machine is routinely Taylor-discharge-cleaned, and the impurity level as monitored by a broadband UV detector indicates a relatively clean plasma. Unless otherwise noted (Section 3.6) the machine is operated without any localized limiters.

The edge plasma, defined here as the region r/a = 0.75–1.0, is diagnosed using Langmuir probes similar to those described previously [6]. The single cylindrical tungsten tip used for most of these experiments has (unless otherwise noted) a radius $r_p = 0.08$ cm, a length of 0.23 cm, and a total exposed area of 0.13 cm^2. This tip is mounted at the end of a 0.35 cm diameter grounded stainless steel shaft and insulated from the shaft by a recessed ceramic sleeve. Variously sized probes of tungsten, gold or stainless steel have been tried, with either grounded or insulated shafts, with essentially the same results. The probe tip is biased typically −150 V with respect to the local chamber ground in order to collect ion saturation current J^+; very similar results are obtained over a range of biases from −100 to −200 V. The probe current is monitored by the voltage across a 3–10 ohm series resistor in the biasing circuit. The voltage at the probe can also be swept to obtain the local electron temperature from the (I,V) characteristic in the usual way [16, 17]. Edge densities and temperatures deduced from the probe data are similar to those obtained for other tokamak edge plasmas [18, 19], i.e. $n \cong (0.5–5) \times 10^{12}$ cm^{-3} and $T_e \cong 15–35$ eV.

The use of Langmuir probes for studying edge-plasma turbulence has some advantages and some disadvantages with respect to the more sophisticated technique of electromagnetic scattering. The main advantages of the probe technique are its extremely good spatial resolution (the probe size is $r_p \cong \rho_s/2$, where $\rho_s = \sqrt{T_e/m_i}/\omega_{ci} \cong 0.15$ cm) and the simultaneous sensitivity of the probe to many wavelengths, particularly to those long wavelengths $k_\perp \rho_s \lesssim 0.3$ which are sometimes difficult to resolve with scattering. Although the probe response will diminish for wavelengths smaller than the tip diameter ($k_\perp \rho_s \gtrsim 6$), the relative fluctuation level for all larger wavelengths can be measured directly without calibrations and calculations such as are necessary for scattering measurements. On the other hand, a single probe as used here cannot provide information on the k-spectrum, only on the frequency spectrum, and it cannot generally be assumed that these two spectra are directly related through a constant phase velocity. Also, the detailed theory of ion collection in a warm magnetized plasma can be very complicated [20, 21], so that the interpretations of the probe signals are always inexact to some extent (see below). Finally, the probe can obviously be operated only in the cold outer regions of the tokamak, and even there an effort must be made to ensure that perturbations due to the probe on its local environment are negligible (see below).

In this experiment the turbulence spectra and relative fluctuation level are monitored using the ion saturation current J^+ (although similar results can also be obtained with the electron saturation current). In general, the ion saturation current to the probe can be written [18, 20]:

$$J^+(\mathrm{A \cdot cm^{-2}}) = I^+/A = ne\bar{v} \qquad (1)$$

where I^+ is the current drawn by the probe, n is the local plasma density, $\bar{v}$ is a velocity characteristic of ions entering the probe sheath, and A is the effective area for ion collection. Thus an estimation of the local n from the measured I^+ involves a knowledge of both A and v. Although the 'small sheath' condition is easily satisfied ($r_p \gg \lambda_D$), the effective A in general depends on the size of the ion gyroradius compared with the probe size. For our case, $r_p \cong \rho_i$, so we use the total exposed area of the tip, i.e. A = 0.13 cm^2, for calculating the average densities. The velocity $\bar{v}$ is usually taken to be the ion sound speed [18], $\bar{v} = (1/4)\sqrt{(8/\pi)\, T_e/m_i}$, and we shall use this formula even though the exact ratio of T_e/T_i is not known for this plasma. The uncertainties involved in estimating A and $\bar{v}$ imply that there is at least a factor-of-two uncertainty in the estimation of the absolute value of density obtained using Eq.(1).

Fluctuations in J^+ can in general be caused by fluctuations in n, $\bar{v}$ or A. Since the sheath is negligibly small and the magnetic fields are approximately constant, we can rule out fluctuations due to A. If the plasma electron (or ion) temperature was fluctuating, this would also cause a fluctuation in J^+ proportional to $\sqrt{\tilde{T}}$. However, we have so far been unable to detect any broadband $\tilde{T}_e$ with a rapidly swept probe (to be reported elsewhere), while there is clear evidence for $\tilde{n}$ from scattering, so we can tentatively assume $\tilde{T}/T = 0$, $\tilde{J}^+ \propto \tilde{n}$ and $\tilde{J}^+/\bar{J}^+ = \tilde{n}/n$. Even if $\tilde{T} \neq 0$, the $\tilde{J}^+$ signal has a precise interpretation in terms of the local ion flux to the probe.

Another possible source of J^+ fluctuation would be obtained if the floating potential of the plasma fluctuated and if the actual slope of the (I, V) probe characteristic in the ion saturation region was not exactly zero. This effect has been estimated for our case by noting that the measured floating potential fluctuations are typically $\tilde{\phi} \lesssim 20$ V (root mean square) about zero, and that the average collected current varies by less than 6% between bias levels of -125 V and -175 V; thus the expected changes in J^+ due to the potential fluctuations around -150 V are less than 2% root mean square and therefore negligible with respect to the observed fluctuation level of 20–80%. This effect can in principle be eliminated by using a double probe to bias one probe with respect to another nearby probe; however, we have chosen to retain the simpler single-probe method in the present experiment.

There is also the possibility that fluctuations in a high-energy electron tail could cause a response in J^+, since these electrons would not be repelled by the probe bias. This effect was shown to be negligible by noting that a probe shielded from the electron drift side has J^+ and $\tilde{J}^+/\bar{J}^+$ similar to an unshielded probe. Secondary electron emission from the probe may also cause the total current to be larger than the ion current; however, as long as the secondary electron emission coefficient is constant, this effect would only change the absolute magnitude of the inferred density and not the relative fluctuation level or spectrum.

Thus we conclude that the fluctuations in the probe current $\tilde{J}^+$ are essentially due to fluctuations in the local plasma density. However, for the sake of precision we retain the notation $\tilde{J}^+$ and $\tilde{J}^+/\bar{J}^+$ rather than translate this measurement into an equivalent $\tilde{n}$ and $\tilde{n}/n$.

Various checks have been made which show that the presence of the probe does not perceptibly change either the global plasma or the local fluctuation level, at least for probes in the cool edge region where the heat load onto the tip is not high enough to evaporate it. For example, the introduction of a second probe <0.2 cm away from a given probe does not change the signals from the first probe, whether or not the second probe is biased. Also, the total UV emission monitored near the probe does not change as the probe is inserted, indicating that the probe is not a significant source of impurities. A separate attempt to bias a very large 2 cm × 7.5 cm 'probe' in the edge plasma showed that up to 10 A of ion current can be drawn from the edge without affecting the global properties of the discharge and without affecting the local fluctuations.

The clearest evidence that the probes do not perturb the plasma comes from a recent measurement of edge turbulence made using the visible light emitted from the edge plasma of the Caltech tokamak [11]. It was shown that the light intensity fluctuations near the probe tip are well correlated with probe $\tilde{J}^+$ signals and that these light fluctuations were unchanged when the probe was removed from the plasma. This again indicates not only that the probe did not perturb the fluctuations, but also that the probe was responding to the same density fluctuations which cause the visible light emission to fluctuate.

Finally, a previous comparison between probe and far-infra-red (FIR) scattering in Microtor [4] showed that the edge fluctuation spectra were the same as those measured by the two systems, but that the probe indicated a higher relative fluctuation level than the scattering system. This disagreement can be accounted for by the difficulties in the calibration of the FIR detector and geometry [22], by the different volume of plasma sampled by the two systems, by the uncertainty in measuring the local $\bar{n}$ for the FIR measurement, and by the uncertainties involved in using the scattering system in the long-wavelength region $k_\perp \rho_s < 0.3$ where the fluctuation amplitude is still very high. On the other hand, the principal uncertainty in the interpretation of the probe $\tilde{J}^+/\bar{J}^+$, namely the possible existence of significant electron temperature fluctuations, still remains a potential contributor to this discrepancy. However, a recent measurement of turbulence in the TEXT tokamak using a multi-channel FIR system [23] has shown edge fluctuation levels to be up to 30%, indicating that the probe and FIR results are not all that different.

The $\tilde{J}^+$ signals are digitized at typically 2 MHz with LeCroy 2264 recorders. The band width of the signal amplifiers is limited to 1 MHz to avoid aliasing. The high-frequency response of the $\tilde{J}^+$ signals is limited only by the effective resistance of the probe and the ~ 100 pF cable capacitance, and is estimated to be well above 1 MHz. This was checked to be so by noting that the cable length could be increased ten times without affecting the observed fluctuation spectrum. The low-frequency response of the probe biasing circuit was set by the discharge of the 1000 μF series capacitor to be $\sim$1 Hz.

Typically, 32 kbytes of 8-bit data were recorded for each shot for later analysis on an LSI 11/23 computer. Spectra are calculated for 1-kbyte-long records using a Hanning window and typically a 6 kHz FWHM Gaussian averaging. Fluctuation levels are calculated by taking the root-mean-square deviation about the mean after linear trend removal and normalizing by the mean.

3. SCALINGS OF EDGE TURBULENCE

Measurements of the edge-plasma turbulence under various discharge conditions are described in this section. A comparison of these results with other experiments and with theory is given in Section 4.

3.1. Time dependence

Figure 1(a) gives an example of a typical tokamak discharge, showing the plasma current, total UV light emission through the plasma centre, line-averaged density $\bar{n}$, and ion saturation current J^+, which for this case was monitored by a probe located at the top of the chamber, 1.5 cm in past the chamber wall (r/a = 0.9). Without gas puffing the average density would stay below 10^{12} cm^{-3} after t = 2 ms; with gas puffing, such as shown, the average density can be raised up to 10^{13}cm^{-3}. In general, the average value of the ion saturation current $\bar{J}^+$ follows the time dependence of the line-averaged density, but the exact shapes of these two signals can be different owing to variability of the density profile and plasma positioning.

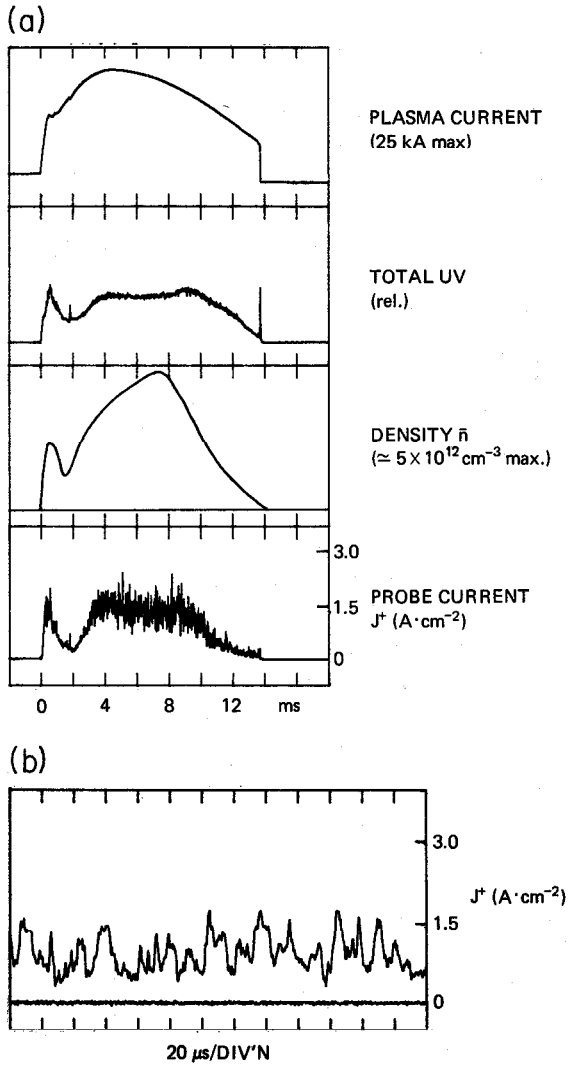

FIG.1. (a) Typical tokamak discharge showing the time dependences of plasma quantities and also the Langmuir probe ion saturation current J^+ measured at r/a = 0.9; (b) expansion of the J^+ trace at t ≅ 8 ms, showing its turbulent character.

Figure 1(b) gives a detailed view of the J^+ trace, which shows the irregular and apparently unpredictable nature of this signal as observed throughout the whole discharge. According to the discussion of Section 2, this signal can be interpreted as the time dependence of the plasma density at the point in space occupied by the probe.

Some analysis of the J^+ signal of Fig.1(b) is given in Figs 2(a, b). The autocorrelation function of $\tilde{J}^+$ shows that a typical autocorrelation time is only ≅ 10 μs and that there are no significant long-time correlations as might be expected for coherent modes (except for the pre-disruptive high MHD phase, as discussed in Section 3.5.6). For this case the amplitude distribution function of J^+ is approximately Gaussian about its mean, as would be expected from a random variable (see Section 3.3).

Figure 2(b) gives an example of the power spectrum of the $\tilde{J}^+$ signal plotted in three different ways. The typical spectra are very broad, extending from ~10 kHz to 1 MHz. The spectral shape can be approximately described as flat up to some critical frequency [3] $f_c \cong 50-100$ kHz, above which the spectral power falls with an approximately power-law dependence $P(f) = f^{-\alpha}$, where for this spectrum $\alpha = 2.5$ in the frequency range 100–1000 kHz. The spectrum might also be described as approximately exponential over the range 10–500 kHz. The linear plot of power versus frequency serves to point out that nearly 90% of the power is below 100 kHz, a fact which is somewhat masked in the log-log plots.

Figure 2(c) gives an analysis of the time dependence of the whole discharge of Fig.1, again for the same probe position r/a = 0.9. The average $\bar{J}^+$ has been translated into a local density using Eq.(1) and the assumption of a constant electron temperature of T_e = 25 eV. The actual temperature measured from the (I,V) probe characteristic is also shown in this figure.

The relative fluctuation level of J^+ is defined as the root-mean-square fluctuation amplitude $\tilde{J}^+$ (after linear trend removal) divided by the mean value $\bar{J}^+$. The values calculated for this discharge and for this probe position are shown to have a range of

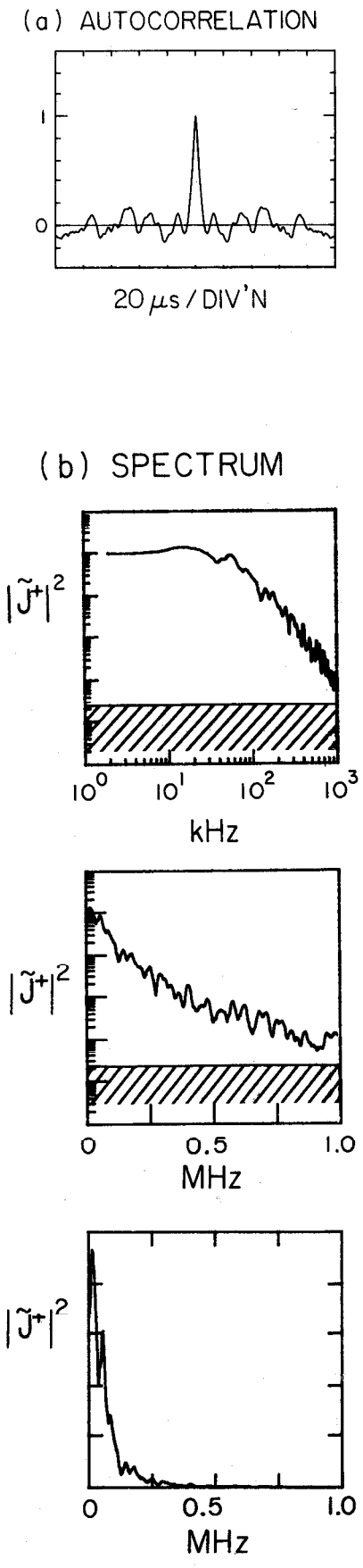

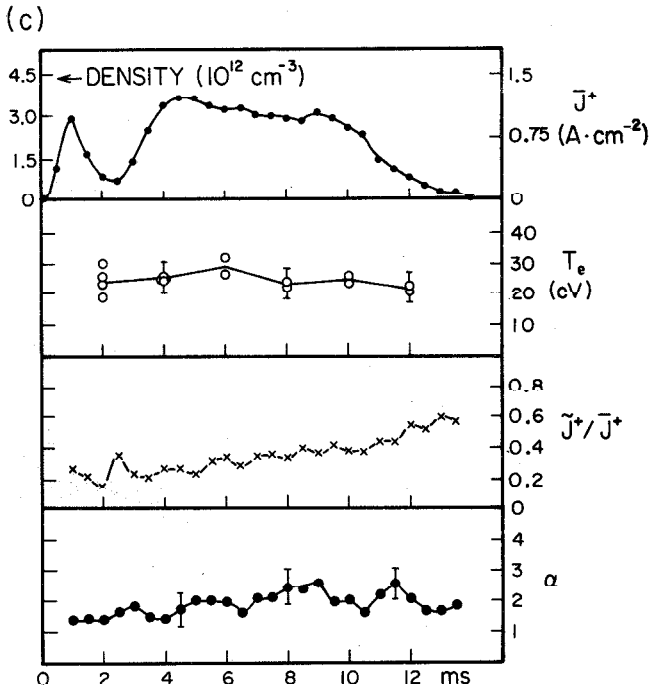

FIG.2. (a) Autocorrelation function of the sample of J^+ in Fig.1(b), showing the short autocorrelation time of 10 μs; (b) typical power spectra of J^+, taken over a 0.5 ms interval at $t \cong 8$ ms, with the same data plotted on log-log, log-linear and linear-linear scales (hatched region shows system noise level); (c) time dependences of various probe quantities for the discharge of Fig.1.

$\tilde{J}^+/\bar{J}^+ \cong 0.15$–$0.6$; however, during the steady portion of t = 4–8 ms the typical value is $\tilde{J}^+/\bar{J}^+ = 0.3$.

The frequency spectrum can be characterized in various ways, for example by its FWHM or by the frequency f_c above which it begins to fall with a power-law dependence. However, since the FWHM is affected if there is a low-frequency coherent MHD mode present (see Section 3.5.6), and since the f_c is not as sharply defined as it might be for the k-resolved spectra, we have instead used the power-law index α in the range 100–1000 kHz as the spectral shape variable. For this typical discharge the power spectrum exponent can be characterized by $\alpha = 2 \pm 0.5$ for all times during the discharge, as shown in Fig.2(c).

Examination of a typical discharge has thus shown the following: The fluctuation level in the edge plasma is always quite large, typically $\tilde{J}^+/J^+ \cong 0.3$, and the spectrum is always quite broad and roughly invariant in shape. At no time during such a typical discharge can the plasma be termed 'stable', either through having a very small relative fluctuation level or a very long autocorrelation time.

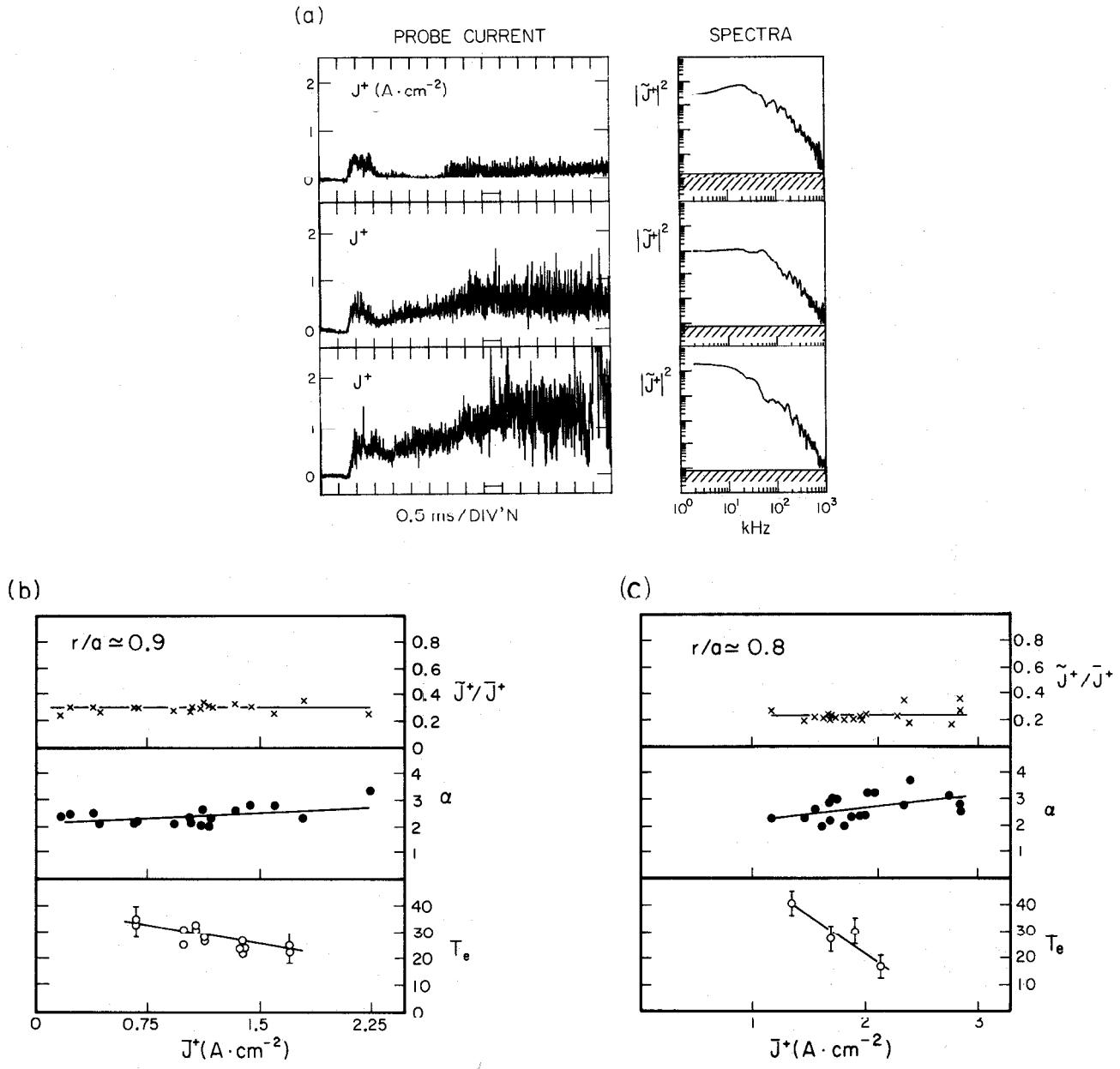

FIG. 3. (a) Traces of J^+ versus time for three different discharges in the density scan, i.e. no gas puffing (top), intermediate gas puffing (middle), and maximum gas puffing (bottom), shown together with the respective spectra at the times indicated by the bars; (b) results of the density scan for a probe position of r/a = 0.9; (c) results of the density scan for a probe position of r/a = 0.8.

3.2. Density dependence

In the previous example it was shown that the spectrum and relative fluctuation level of J^+ were roughly invariant with time during a typical discharge. To examine the density dependence of the turbulence, a scan was made of the gas puffing strength (and hence the density) while keeping all other parameters fixed. The probe was again inserted from the top of the chamber.

Figure 3(a) gives some data from a density scan for which the probe was at r/a = 0.9 (as for Figs 1 and 2). At the top is J^+ versus time with no auxiliary gas puffing ($\bar{n} = 10^{12}$ cm^{-3}), and at the bottom the disruptive density limit was reached at t = 7 ms owing to strong gas puffing. Therefore, this scan covers the full

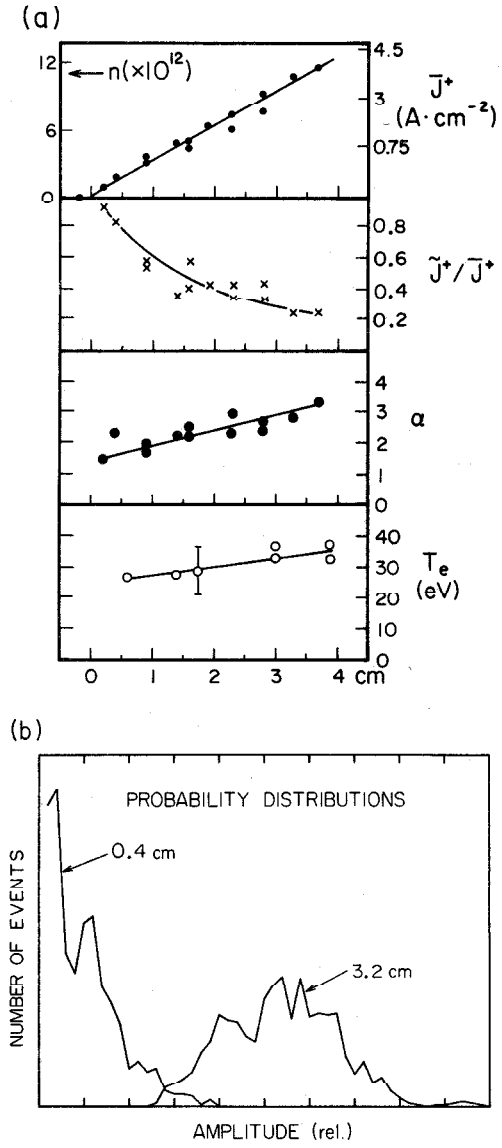

FIG.4. (a) Radial profiles from a probe scan, showing the decrease in relative fluctuation level toward the plasma centre; (b) probability distributions of the amplitude of J^+ for two probe positions in this scan.

density range available on this machine, over which the local average ion saturation current $\bar{J}^+$ varies by a factor of 10 (at t = 4 ms). Note that the plasma current which peaks at t = 4 ms decreases by only 15% with increasing density over this range.

Power spectra of $\tilde{J}^+$ analysed at the time indicated by the bars (t = 4 ms) are shown on the right of Fig.3(a). Evidently, the spectral shape is not a sensitive function of the local density.

In Fig.3(b) the relative fluctuation level and spectral index are plotted versus the average $\bar{J}^+$, again for the time t = 4 ms. There is no systematic change in $\tilde{J}^+/\bar{J}^+$ with density over this range at this position, while there is at most a slight increase in α with increased $\bar{J}^+$. Local electron temperatures are also shown for part of this scan; since T_e is decreasing with $\bar{J}^+$, the local density as inferred through Eq.(1) is changing by approximately a factor of 15 over this range of $\bar{J}^+$ ($3 \times 10^{11} - 5 \times 10^{12}$ cm^{-3}).

Figure 3(c) shows a similar scan, but this time for a probe position of r/a = 0.8 instead of 0.9 as above. Although the $\bar{J}^+$ values are somewhat higher and the fluctuation levels are somewhat lower (see Section 3.3), there is again no systematic variation in $\tilde{J}^+/\bar{J}^+$ with density in this case.

3.3. Radial dependence

The radial dependence of the $\tilde{J}^+$ fluctuations is obtained by varying the probe position, keeping all other parameters fixed. The discharges used were of a relatively high-density type, with $\bar{n} = 10^{13}$ cm^{-3}. The probe was again inserted from the top into a limiterless chamber, and no change in the global discharge parameters was caused by the insertion of this probe up to r/a = 0.75.

The radial profile of $\bar{J}^+$ and its root-mean-square fluctuation level are shown in Fig.4(a), together with the spectral index and the electron temperature. This profile was taken at t = 6 ms for this case, but similar results are obtained for other times and at other line-averaged densities. The average value $\bar{J}^+$ varies by over an order of magnitude in this radial scan, while T_e changes by only 30%. The local probe density as calculated using Eq.(1) is shown on the left-hand scale, where the approximation has been made that $T_e = 30$ eV throughout this region.

This figure shows that the relative fluctuation level decreases significantly from a maximum of 0.9 near the wall to a minimum of 0.2 at the point farthest into the plasma. This is the most pronounced variation in $\tilde{J}^+/\bar{J}^+$ seen for any scan within the normal operating range of this tokamak. The spectral index also increases significantly from 1.5 near the wall to 3 at r/a = 0.75.

The amplitude distributions of the J^+ signals near the end-points of this scan are shown in Fig.4(b). At places where the relative fluctuation level is about 0.2 the distribution function has a symmetrical Gaussian-type distribution about its mean; however, nearer the wall where the fluctuation level is 0.8 the distribution function becomes strongly skewed. It is clear that in the latter case the plasma does not simply have a small density fluctuation about a mean, but rather has

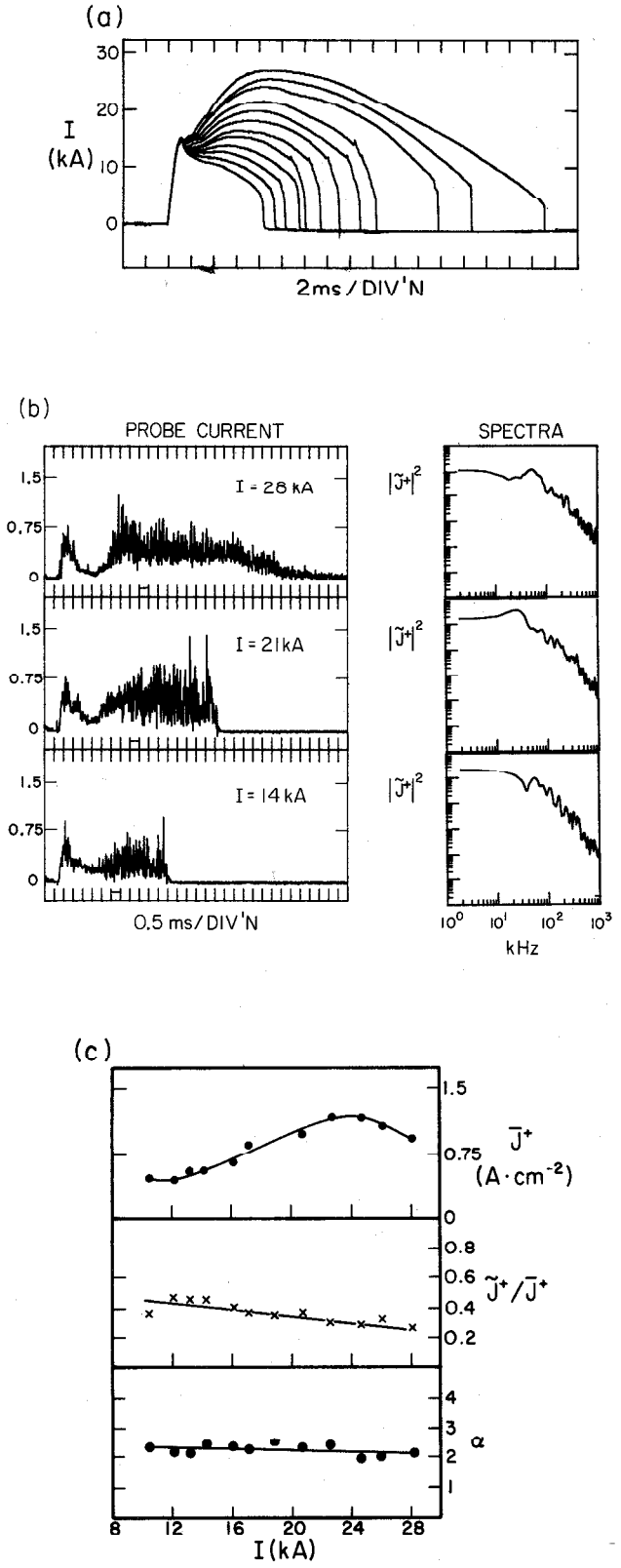

FIG.5. (a) Plasma current traces for the current scan; (b) probe J^+ signals and spectra for three different plasma currents (spectra taken at the bars); (c) results of the current scan.

a 'shredded' structure in which one can imagine that discrete shreds of plasma (elongated in the toroidal direction) interact with one another rather than with the average background.

3.4. Current dependence

The plasma current was varied at fixed toroidal field by adjusting the Ohmic heating voltage and keeping the gas puffing and all other fields at their normal values. The standard probe was used at a position r/a = 0.9 at the top of the chamber. Since the toroidal field was 3.5 kG, the resulting current range of 10–28 kA represented a range of q (a) = 3.3 – 9.

The current wave forms in Fig.5(a) show that the discharge length also shortens significantly as the voltage is reduced; therefore, many plasma parameters (i.e. average density and temperature) are changing together with the current in this scan and so we cannot unambiguously determine the current dependence of the edge stability. However, it can be seen from Figs 5(b), (c) that in all cases the J^+ fluctuations (at peak current) were large and turbulent, independent of the plasma current over this range.

The plasma current also varies at the beginning and end of a discharge. In these circumstances also there is no qualitative change in the character of the turbulence in the edge plasma (see, for instance, Fig.8(b)). Thus we can tentatively conclude that plasma current is not an important variable in determining the edge stability; however, the range of variation of the local current density during these scans is not known.

3.5. Other dependences

Several other dependences were investigated which basically confirm the notion that the edge turbulence is relatively invariant with respect to changes in the plasma conditions. The following results were all obtained using the standard probe inserted from the top of the chamber at r/a = 0.9, unless otherwise noted.

3.5.1. dn/dt dependence

A specially programmed discharge was produced in which strong gas puffing was started at t = 3 ms and stopped at t = 7 ms, so that the time-dependent behaviour of the edge fluctuations during density rise and fall could be examined. Between t = 3 ms and t = 7 ms the average ion saturation current at the probe J^+ rose by a factor of 5; between t = 4.5 ms and t = 7 ms, J^+ was approximately constant, and from

t = 7–10 ms, J^+ fell again by a factor of 4. Over this whole time the relative fluctuation level remained nearly constant at $\tilde{J}^+/J^+ = 0.25 \pm 0.05$, with no systematic trends toward increasing or decreasing with dn/dt. The spectral coefficient also remained within its normal range over this time period. Thus the scaling with density obtained in this way was quite similar to that obtained by varying the steady-state density as described in Section 3.2.

This constancy of the relative fluctuation level is in part similar to results obtained in PLT during a similar density-rise experiment [24], in that in PLT the relative fluctuation at the edge was the same before and after an increase in edge density. However, a transient increase in fluctuation level during the period of largest dn/dt observed in PLT was not observed in the present experiment, which is perhaps due to the considerably different neutral penetration length relative to the chamber size (i.e. the ion source function is much more peaked toward the edge in PLT).

3.5.2. Poloidal dependence

Edge turbulence levels and spectra were measured at both the outer equatorial plane and the inner equatorial plane (R = R ± a), and results very similar to those measured from the top (Fig.4) were obtained. An example of a radial scan made from the outer equatorial plane is shown in Fig.7(b).

A separate attempt was made to compare the probe J^+ signals from the inner and outer equatorial planes for the same discharge. It was found that when the average $\bar{J}^+$ was the same for these two probes, the spectra and relative fluctuation levels were also approximately the same. Thus there is evidently no strong poloidal dependence of the edge turbulence in this tokamak.

3.5.3. Position dependence

Since the plasma position is not feedback-controlled in the present experiment, and since this position would be expected to change somewhat with changing density or current, separate scans were made to determine the dependence of the edge turbulence on the radial plasma position. This was done by varying the applied vertical field at a fixed density or at a fixed current.

The result was that the relative fluctuation level and spectrum of J^+ were approximately unchanged over the range of vertical fields which produced normal discharges. This indicates that the edge fluctuations are not sensitively dependent on the particular way in which the plasma contacts this limiterless chamber. Note that the top probe position is less sensitive to in/out positioning than a side probe (top probes were used for the parameter scans of Sections 3.1–3.4).

3.5.4. Toroidal field dependence

The magnitude of the toroidal field B_T was varied over the range 2.3–4.6 kG while keeping all other external parameters constant (normally, $B_T = 3.5$ kG). It was found that the spectra had their usual form, $\alpha = 2$–3, over this whole range; however, there was a trend for the relative fluctuation level to decrease with increased B_T over this range (by about a factor of 2). Unfortunately, the plasma current and density were also varying as the toroidal field varied, so that this trend could not be unambiguously related to the toroidal field.

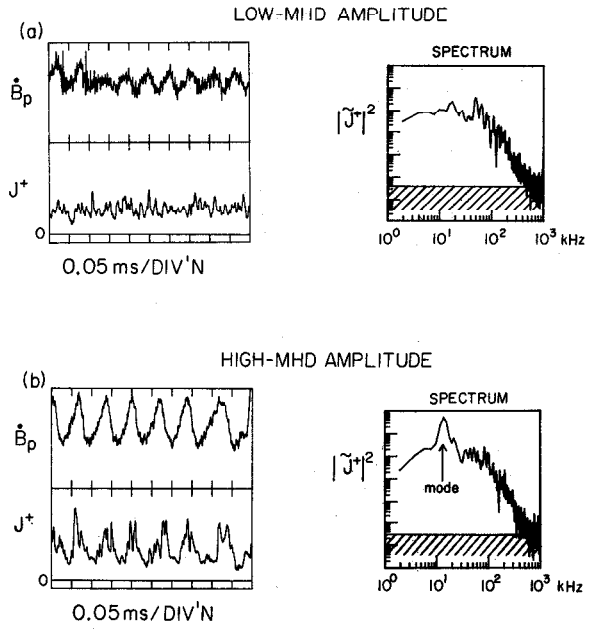

FIG.6. Langmuir and magnetic probe signals and spectra for two different MHD activity levels: (a) low level during a normal discharge, and (b) high level later in the same discharge just preceding a major disruption. The MHD mode can be seen at 15 kHz in the J^+ spectrum in case (b); however, the rest of the turbulent spectrum is unchanged (1 kHz FWHM frequency averaging was used for these spectra).

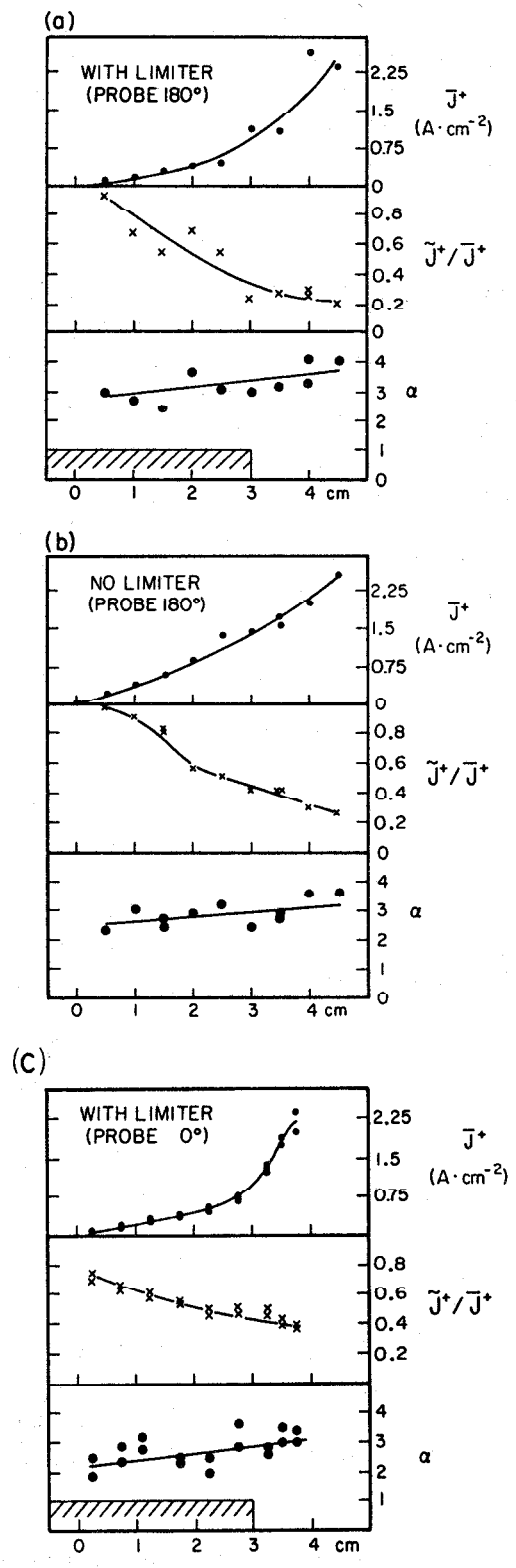

FIG. 7. (a) Radial profiles taken 180° toroidally away from an outer limiter; (b) same profiles but with the limiter removed; (c) radial profiles taken with a probe directly adjacent to the outer limiter. These results show that the turbulence in the shadow of a limiter is similar to that observed in the edge without a limiter.

3.5.5. Impurity level dependence

A comparison was made between the edge turbulence in a normally discharge-cleaned plasma and that obtained in dirtier plasmas without proper cleaning (the impurity involved was predominantly oxygen from the walls). The impurity level was increased to the point where the discharge was significantly degraded, i.e. the plasma current decreased by more than a factor of 2, while the total UV radiation (from impurities) increased by more than a factor of 10. Over this range of impurity levels the edge turbulence spectrum was qualitatively unchanged and the relative fluctuation level varied by less than a factor of 2. This result again shows that edge turbulence occurs over a wide range of plasma conditions, in particular over a wide range of edge collisionality.

3.5.6. MHD dependence

In this tokamak there can be large MHD oscillations as the density limit is approached, particularly just preceding a major disruption. Figure 6 is a comparison of two probe J^+ signals, one obtained with the usual low-level MHD activity and the other taken 1.5 ms later in the same discharge during high-level MHD activity just preceding a major disruption. Also shown are $\tilde{B}_p$ signals from a magnetic probe located at the wall.

Evidently, the Langmuir probe does respond to the high-level MHD mode, as can be seen particularly by the narrow peak in the $\tilde{J}^+$ spectrum at 15 kHz for this case. This type of response would be expected from a density modulation caused by the rotating magnetic island. However, it can be seen that the rest of the $\tilde{J}^+$ spectrum above 20 kHz is not changed by the presence of this coherent mode, which suggests that MHD and edge turbulence can be superimposed without qualitatively affecting the turbulence.

3.6. Limiter dependence

For all the above cases there was no localized limiter in the chamber. The influence of a limiter on the edge turbulence was checked by inserting at the outer equatorial plane a 7.5 cm high stainless steel limiter 3 cm into the chamber. Edge fluctuations were first measured with the standard probe located 180° toroidally away from the limiter at the outer equatorial plane. The discharges were of the typical kind shown in Fig.2, and the data were analysed for the steady-state region at $t \cong 6$ ms.

In Fig.7(a) the observed radial profiles of $\bar{J}^+$ and $\tilde{J}^+/\bar{J}^+$, and the spectral index are plotted for the limiter-inserted case. The radial location of the limiter is shown by the hatched box at the bottom of the figure. For comparison, another scan was made using the same gas puffing and magnetic fields, but with the limiter removed, as shown in Fig.7(b). The presence of the limiter changes the edge density in its shadow, as shown by a comparison of the $\bar{J}^+$ profiles; however, the relative fluctuation levels and spectra at r/a = 0.75–1.0 are the same in both cases. This result is independent of whether the limiter is floated or grounded to the chamber.

A separate run was made to measure the turbulence near to the limiter. A limiter similar to that described above was again inserted 3 cm into the chamber, but this time a probe 0.2 cm long by 0.1 cm diameter was scanned radially in the region directly adjacent to the ion drift side of the limiter (< 0.5 cm toroidally away from the limiter face). The results of this scan are plotted in Fig.7(c). It can be seen that the turbulence in front of the leading edge of the limiter (3.0–3.8 cm from the wall) is quite similar to that observed in the scrape-off region behind the leading edge of the limiter (2.0–3.0 cm from the wall), and that the radial profile of the turbulence next to the limiter in Fig.7(c) is similar to that observed 180° away from the limiter in Figs 7(a, b). The data in Fig.7(c) were taken with the limiter electrically grounded to the wall; however, the results are almost identical for an electrically floated limiter. Thus the presence of an outer limiter does not seem to significantly influence the edge turbulence.

In another set of experiments (to be reported elsewhere) the edge turbulence was also seen to be roughly independent of a bias of ±60 V applied to this limiter, at which point up to 10 A of ion current or 100 A of electron current was drawn by the limiter. Furthermore, the turbulence was also qualitatively unchanged by the presence of a strong local toroidal divertor [25] which was mounted inside a limiter such as that of Figs 7(a, c).

3.7. Filling-pressure dependence

A final scan was made of the initial neutral hydrogen pressure which fills the chamber before the shot. All other external parameters were kept at their normal values. Ordinarily, the filling pressure is fixed at the optimum breakdown point and is not an interesting variable in tokamak operation. However, in this machine it was observed that at an unusually high filling pressure the edge plasma was quite stable, although the discharges themselves were substantially degraded.

Figure 8(a) shows what happens to the plasma current and UV emission when the filling pressure is raised from its normal value of 1.63×10^{-4} torr H_2 (high-current case) to 3.85×10^{-4} torr (intermediate-current case) or to 5.44×10^{-4} torr (smallest-current case). The extra gas in the chamber inhibits the growth of the current, perhaps because of the extra energy loss due to neutral hydrogen radiation. The UV signals indicate a strong increase in total radiation between the normal filling pressure case and the intermediate pressure case; however, at the highest pressure the UV emission drops again as if the plasma was being quenched by the neutrals.

Figure 8(b) shows the traces of J^+ as monitored by the standard probe at r/a = 0.9 at the top of the chamber (note the expanded time-scale). At normal filling pressure the turbulence begins almost immediately and continues at high relative levels with the usual spectrum throughout the current rise phase. At intermediate pressures the magnitude of $\bar{J}^+$ is increased by a factor of 2, but the higher-frequency fluctuations appear to be absent. Finally, at the highest pressures there is only a very low frequency oscillation during the rise of J^+, and there are almost no fluctuations during the decay of J^+. The oscillations on the rising part are not always as coherent as those shown in the figure, but the absence of fluctuations on the decaying part of J^+ is quite reproducible.

Some further properties of this pressure scan are shown in Fig.8(c), where various quantities have been measured at the time indicated by the bars in Fig.8(b). The average $\bar{J}^+$ peaks at about 4×10^{-4} torr, reflecting a competition between the increase in available ion density and the decrease due to loss of ionization at high pressure. The edge electron temperature drops monotonically with pressure to an estimated 5 eV in the stable case at 5×10^{-4} torr, at which point the estimated edge density is 3×10^{12} cm^{-3}. The relative fluctuation level also decreases monotonically with pressure down to less than 3% (some of which comes from the system noise level). An indication of the change in the spectrum is given by the relative amount of fluctuation power in a narrow band around 100 kHz, which seems to drop abruptly above a critical filling pressure.

Magnetic fluctuations were also monitored by a $\tilde{B}_p$ probe in the edge plasma for various filling pressures. At normal pressure the magnetic fluctuations are relatively large and chaotic during the current rise

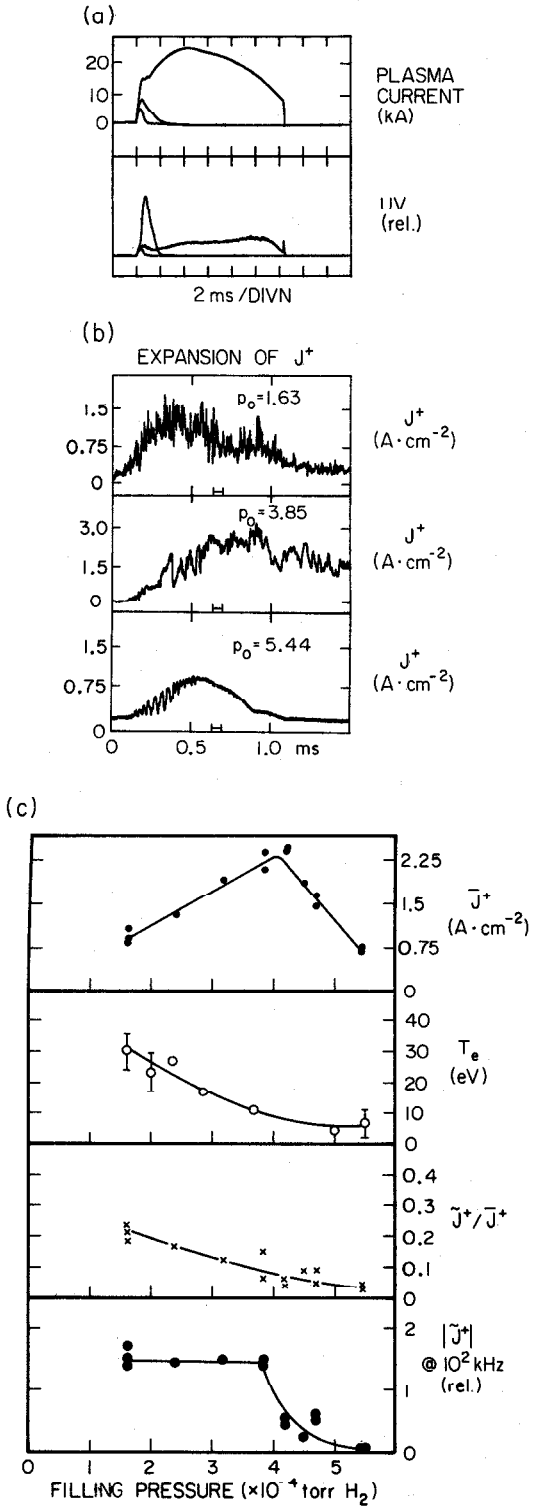

FIG.8. (a) Plasma current and UV emission for three different filling pressures of hydrogen: longest discharge at normal filling pressure of 1.63 X 10^{-4} torr, 2 ms long discharge at 3.85 X 10^{-4} torr, and shortest discharge at 5.44 X 10^{-4} torr; (b) traces of J^+ for these three discharges, showing the unusual edge stability at high filling pressure; (c) results from the filling pressure scan.

portion of the discharge. As the pressure was increased the amplitude of the magnetic fluctuations decreased, and at the highest pressures there were no detectable magnetic fluctuations. Thus there was no coherent $\tilde{B}_p$ present corresponding to the coherent $\tilde{J}^+$ signal seen at the bottom of Fig.8(b).

A more complete analysis of this transition from coherence to turbulence is beyond the scope of the present paper. Some discussion of this stable regime is given in Section 4.5.

A practical consideration should be noted: when operating at an unusually high filling pressure it is possible to create dangerous runaway electron discharges. In the present experiment the hard X-ray flux was carefully monitored, and no runaways were created.

4. DISCUSSION

In this section we first discuss the observations of Section 3 in terms of two commonly cited dimensionless parameters; then a comparison is made with other experimental results on edge-plasma turbulence and with various instability theories. The last subsection is a brief discussion of the stable regime.

4.1. Dependence on collisionality

Figure 9 is a plot of the observed $\tilde{J}^+/\bar{J}^+$ versus the local collisionality as estimated from the probe-inferred density and electron temperature:

$$\frac{\nu_{ei}}{\nu_{Te}} = \frac{4.5 \times 10^{-5}\, n Z T_e^{-3/2}}{v_e/(q(a)\, R_0)} = \frac{q(a)\, R_0}{\lambda_{mfp}} \qquad (2)$$

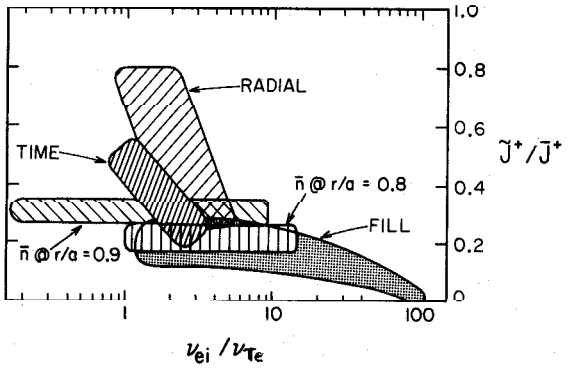

FIG. 9. Relative fluctuation level versus local edge collisionality for various scans. The parameter ν_{ei}/ν_{Te} is the electron collision frequency normalized to the electron transit time.

where λ_{mfp} is the electron mean free path, T_e(eV) is the local electron temperature, n (cm^{-3}) is the local density, and ν_{Te} is the local electron transit frequency taken to be the electron thermal speed divided by the typical parallel scale length q(a) R_0. We have assumed Z = 2 for the purpose of evaluating the collisionality. Each box in Fig.9 represents a particular set of data from Section 3; for example, the 'time' box includes the data described in Section 3.1 on the variation with time during a typical discharge, and the 'radial' box refers to the data described in Section 3.3 on the radial scan. It should be noted that several variables may be changing during each particular scan; for example, in the $\bar{n}$ scans, part of the variation in collisionality is due to the decrease in temperature with increased density.

Evidently, a wide variation in collisionality has been obtained in the edge plasma in this machine; in particular, the '$\bar{n}$' scan at r/a = 0.9 (Section 3.2) shows that the relative fluctuation level is approximately insensitive to the local collisionality over a factor of at least 50. On the other hand, it is also true that at the normal collisionality of $\lesssim 1$ the fluctuation level can vary from 0.2 to 0.8, evidently depending on some other parameters besides collisionality. Therefore, these results imply that the relative edge fluctuation level is not simply determined by the local collisionality.

It should be noted that the systematic uncertainties involved in the calculation of ν_{ei}/ν_{Te} were not included in the boxes of Fig.9; thus the actual numerical value for ν_{ei}/ν_{Te} is uncertain by at least a factor of 2, because of the assumption of Z = 2 and the systematic uncertainty involved in using Eq.(1) to infer the local plasma density.

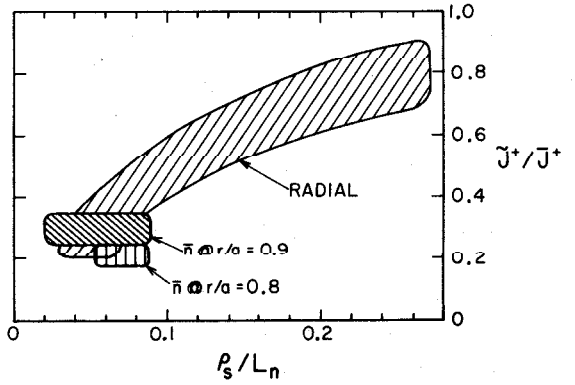

FIG.10. Relative fluctuation level versus local radial scale-length parameter for various scans. The parameter ρ_s/L_n is the ion gyroradius (evaluated at T_e) normalized to the radial density scale length.

For all cases shown in this plot the tokamak was operated without a localized limiter. However, the invariance of the turbulence in the presence of a limiter (Fig.7) also suggests that collisionality is not a significant factor in determining the relative fluctuation level, since the presence of a limiter would appear to strongly affect the electron collisionality in its shadow.

The 'fill' box in Fig.9, referring to the data of Section 3.7, points out a possible explanation for the unusual stability at high neutral pressure, namely that the collisionality is over 10 times its normal value. However, this is only one of several dimensionless parameters which may cause this stability (see Section 4.5).

4.2. Dependence on radial density scale length

Figure 10 is a plot of the observed $\tilde{J}^+/\bar{J}^+$ versus the radial scale-length parameter ρ_s/L_n, where ρ_s is the ion gyroradius evaluated at the electron temperature and L_n is the density-gradient scale length $L_n = n/(dn/dx)$. The 'radial' box again refers to the radial scan of Section 3.3, and the '$\bar{n}$' boxes again refer to Section 3.2. In each case, ρ_s was evaluated using the local probe-inferred temperature measurements and the toroidal field at $R = R_0$.

For the 'radial' scan the variation in ρ_s/L_n comes almost entirely from the change in n versus radius and not from changes in dn/dx or in ρ_s (the temperature profile is very flat in this region). Thus these data reflect the fact that the relative fluctuation level decreases as the probe is moved inward to higher-density regions.

For the '$\bar{n}$' scans the L_n were measured separately at several $\bar{n}$ values by scanning the probe radius ±0.5 cm about r/a = 0.8 or 0.9. For r/a = 0.9 it was found that L_n varied from (2 ± 0.5) cm at $\bar{J}^+ = 0.45$ A·cm^{-2} to L_n = (5.5 ± 2) cm at $\bar{J}^+ = 1.6$ A·cm^{-2}, while for r/a = 0.8 it was found that L_n = (2.3 ± 0.5) cm at $\bar{J}^+ = 2$ A·cm^{-2}. Thus for these data there was not a significant change in the relative fluctuation level even though the ρ_s/L_n parameter varied by about a factor of 2.

However, according to Fig.10 the values of $\tilde{J}^+/\bar{J}^+$ observed in these scans can be approximately given by:

$$\tilde{J}^+/\bar{J}^+ \cong (3-5)\rho_s/L_n \qquad (3)$$

Since there are considerable uncertainties, as indicated by the boxes, the exact form of this scaling is not yet clear; for example, a relationship $\tilde{J}^+/\bar{J}^+ \cong 1.6\sqrt{\rho_s/L_n}$ fits the data at least as well as the linear dependence of Eq.(3). It should also be noted that other variations

are not ruled out by such a scaling; for example, possible changes in temperature gradients or magnetic shear or current density may be occurring together with the explicit changes in radial position and density. Therefore the scaling of Eq.(3) should be considered a tentative correlation rather than a causal connection.

Nevertheless, the results of Fig.10 are similar to the scalings proposed by Mazzucato [1], Horton [26], and Surko and Slusher [12] to fit the range of fluctuation data gathered from different tokamaks. Their scaling of $\tilde{n}/n = 1/k_\perp L_n$ is approximately equivalent to Eq.(3) if we take $k_\perp \rho_s \cong 0.3$, as is typical for drift-wave turbulence, where $k_\perp$ is the mean wavenumber perpendicular to the magnetic field.

There is unfortunately a limitation in these scalings in that L_n is not easily computable from theory, since it depends on the particle diffusion caused by the turbulence and on the particle sources. There is also some question as to the relevance of the average density scale length for regions in which $\tilde{J}^+/J^+ \gtrsim 0.3$ locally, since the instantaneous density gradients are much different from their average values. However, such scalings are at present the only empirical guidelines available to describe tokamak turbulence levels.

4.3. Relation to other experimental results

Langmuir probe measurements of tokamak edge plasmas have been reported previously several times. The most detailed results were from Macrotor in which electron [6] or ion [19] saturation currents were monitored in the edge with and without limiters. The observed edge turbulence was generally similar to that described here; for example, the relative fluctuation levels were always largest nearer the wall and decreased toward the centre of the discharge, the spectra were always broad and turbulent, and the results were independent of the presence of a limiter. However, for Macrotor the relative fluctuation levels were somewhat less than in the present experiment, varying from 40% to 10% root mean square, compared with 80% to 20% in the present experiment, and the spectra of Macrotor fluctuations were also somewhat narrower, with a typical power-law exponent of $\alpha = 4$ compared with $\alpha = 2-3$ in the present experiment. The most significant difference between Macrotor and the present experiment is in the scaling of the relative fluctuation level with density, which was $\tilde{J}^+/\bar{J}^+ \propto n^{-1/2}$ in Macrotor but is $\tilde{J}^+/\bar{J}^+$ independent of density in the present experiment. The reason for this difference is not yet understood.

Other Langmuir probe edge measurements in JFT-2a [8] and DITE [9] have also indicated large levels of $\tilde{J}^+/\bar{J}^+$ in the range of 5–100% with broadband spectra. Also, recent probe measurements on the PRETEXT tokamak [27] and on ISX-B [28] have shown edge turbulence quite similar to that described here. For example, the fluctuation levels in PRETEXT range from $\tilde{n}/n = 0.2-0.9$, while those in the ISX-B scrape-off region are typically $\tilde{n}/n = 0.5$. In both these cases and also in the UCLA [19] Caltech tokamak [7], these edge density fluctuations have also been associated with large edge particle diffusion coefficients, e.g. $D \cong 5D_{Bohm}$ in ISX-B [28].

Another view of the plasma edge was obtained in ASDEX [10] by using a high-speed movie camera focused on the visible light emitted from the hydrogen in the edge. Relatively small-scale 'filaments' were observed which were irregularly fluctuating in space and time. A connection between these visible light fluctuations and the Langmuir probe $\tilde{J}^+$ fluctuations was established using a visible photodiode array in the Caltech tokamak [11].

Finally, several types of electromagnetic scattering experiments have shown that broad frequency and wavenumber density turbulence exists in the edge plasma, with frequency spectra (averaged over $k_\perp$) which are generally similar to those seen in the present experiment. Also, the relative fluctuation levels are seen to increase toward the wall as in the present experiment. In particular, the CO_2 scattering results [2] have consistently indicated that edge fluctuation levels are typically in the range of 10–100%. Using millimetre scattering, the relative fluctuation levels have been estimated to be 2–5% at $r/a \cong 0.8$ [1, 3] rather than the $\gtrsim 20\%$ as reported in the present experiment; however, a recent result from multi-channel FIR scattering in TEXT [23] also indicates a $\gtrsim 20\%$ fluctuation level. These differences may in part be due to the differing plasma conditions; however, some of the difference may be due to the presence of very long wavelength components ($k_\perp \rho_s \ll 1$) which are difficult to resolve with some scattering systems (see Section 1).

4.4. Relation to theoretical models

Instabilities driven by density or temperature gradients are plausible candidates for explaining the observed edge turbulence, since the presence of particle and energy sources and sinks allows relatively large gradients to form in the edge region. Other possible sources of instability refer more directly to the presence of the open-flux surfaces intersecting the wall or limiter,

or to the particularly low electron temperature or directed velocity of the plasma near the wall.

Hasegawa and Wakatani [29] have calculated the non-linear mode coupling of collisional drift waves in a shearless slab fluid model and have shown that a strongly turbulent saturated state exists in which density fluctuation levels can be as high as 30% and for which there is a broad frequency and $k_\perp$ spectrum. The main parameter determining the saturated state was ρ_s/L_n. These results appear to be at least qualitatively consistent with typical results in the present experiment, e.g. the edge plasma is usually fairly collisional, the fluctuation levels inferred from the probe data were typically 30%, the frequency power spectrum exponent was similar to the $k_\perp$ power spectrum exponent, and ρ_s/L_n was a parameter useful in describing the trends in the data. However, in the present experiment it was observed that the edge turbulence appeared to persist even into the collisionless regime where the approximations of the Hasegawa model break down. One possible resolution would be that turbulence is convected radially such that a collisionless point is being influenced by the turbulence from a more collisional point (in this tokamak there is a range of radii in the edge region over which the collisionality increases toward the centre of the plasma).

Terry and Diamond have recently described an analytic calculation of the spectrum of dissipative drift-wave turbulence in a tokamak edge plasma [30]. Their results agree at several points with the data presented here; for example, the calculated fluctuation amplitude for a typical collisional edge plasma was $\tilde{n}/n \cong \sqrt{3}\rho_s/L_n$, which is about a factor of two below the results of Fig.10, and the calculated $\tilde{n}/n$ was also seen to be approximately invariant with collisionality (in the collisional regime), in agreement with the results of Fig.9. In addition, the calculated frequency spectrum was broad and peaked at low frequencies similar to the data presented here. The calculated radial particle diffusion also scaled as $D \propto n^{2/3}T^{1/6}$, in qualitative agreement with recent probe data from PRETEXT [27].

Several other models of drift-wave turbulence have been developed which are not necessarily specific to the collisional edge region [31–35]. In particular, Waltz and Dominguez [32] have calculated broadened spectra with a saturated turbulence level, $\tilde{n}/n \cong 2\text{–}5\ \rho_s/L_n$, which is only weakly dependent on the driving strength of the instability, while the resulting transport was found to be linearly dependent on the driving strength of the instability. In general, these models are each investigating one or more of the many possible driving and damping mechanisms which may be responsible for producing the saturated steady-state turbulence observed in the experiments.

Another type of instability due to temperature gradients has been investigated by Callen et al. [36] and Carreras et al. [37]. They have shown that under typical tokamak edge conditions the rippling mode is unstable, and have calculated the linear, non-linear and turbulent phases of this instability in the context of resistive MHD theory. Good agreement has been obtained between their model and the edge fluctuation correlation lengths in Macrotor, and these models also predict broad spectra and short autocorrelation times as seen in the experiments. However, the calculated relative fluctuation levels of 5–10% appear to be too low to explain the 20–40% levels observed both in Macrotor and in the present experiment.

Since both the collisional drift and rippling mode models predict edge density turbulence, it is not yet clear which (if either) instability dominates in the present context. Hassam and Drake [38] have shown that there is a smooth transition from one mode to the other, depending on the collisionality and current density. For typical parameters of the present experiment (i.e. from the radial scan of Fig.4(a) at 2 cm) we find $\hat{J} \cong 0.5$ and $\hat{C} \cong 1$ in the normalized units of Ref. [38]. Although this result implies instability in the collisional-drift region, a factor-of-three increase in $\hat{C}$ would move the plasma into the rippling region, and this cannot be ruled out considering the uncertainties in the plasma parameters. On the other hand, the rippling instability can also be viewed as having an electron temperature threshold above which it is stable, and according to Ref. [38] this threshold can be as low as $T_e \cong 5$ eV for typical edge plasma conditions in the present experiment. However, the linear model of Hassam and Drake may not be directly applicable to the strongly turbulent plasma observed in the present experiments.

A model implicating the limiter as a possible source of edge turbulence has been described by Staib [18], and a somewhat different limiter model has been discussed by Motley [39]. These authors point out that the equilibrium and stability of a plasma on open field lines intersecting a limiter may be quite different from those of a confined plasma, particularly with respect to the creation of d.c. electric fields which can drive convective plasma flows. However, the results of Fig.7 show that the edge turbulence appears present with or without a localized outer limiter. Furthermore, the vertical field scan of Section 3.5.3 shows that in the limiterless case the turbulence was also insensitive to the plasma location within the chamber. It remains

possible that even a nearly parallel contact of the field lines with the wall is enough to form a turbulent boundary, perhaps indirectly through plasma flows [40] or radial electric fields [41].

Considering the wide range of experimental parameters over which the plasma edge is strongly turbulent, one would suspect that the appropriate theoretical models would predict saturated states which were not sensitive to the details of the linear growth or damping mechanisms. This is in fact the case for several non-linear models; however, this also makes the identification of the 'source' of the instability quite difficult. Another difficulty in comparing experiment and theory lies in the possibility that the turbulence is convected either inward from the edge or outward from the centre, in which case the local parameters do not necessarily determine the local turbulence.

4.5. Stable edge state

The unusually stable regime observed at high neutral filling pressure (Fig.8) may not exist in 'normal' tokamak discharges, but it does show that a toroidal current-carrying plasma need not be turbulent. The stability may be related to the very high collisionality or to low ρ_s/L_n obtained in this cold and rather high-density plasma (Fig.9); however, other dimensionless parameters may be involved, such as the streaming parameter, magnetic shear, temperature gradients, etc.

It is interesting to note that there is a smooth transition between a coherent mode and an incoherent turbulent spectrum as the discharge comes nearer to a normal neutral filling pressure. A further investigation of the coherent state may allow an identification of the dispersion relation and the driving terms which ultimately lead to the turbulence.

Finally, the non-turbulent and relatively stable edge state observed under these conditions might have some connection with the recently observed 'H-mode' [42] plasmas which appear in certain diverted tokamaks. If edge-plasma conditions like those observed in this tokamak at high neutral pressure are being reproduced in the edges of larger 'H-mode' tokamaks, then their improved edge stability might help explain the overall improvements in particle and energy confinement.

5. SUMMARY

Edge-plasma stability has been studied over a wide range of parameters in the Caltech research tokamak. The relative fluctuation levels and spectra were measured by the ion saturation current J^+ drawn to small metal probes inserted into the plasma edge. The results were as follows:

(1) The relative fluctuation levels were typically $\tilde{J}^+/\bar{J}^+ \cong 0.2$–$0.8$ in the edge plasma. The clearest variation in the relative fluctuation level correlates with the probe's radial position in the plasma, i.e. $\tilde{J}^+/\bar{J}^+ \gtrsim 0.8$ at $r/a \cong 1$ while $\tilde{J}^+/\bar{J}^+ \cong 0.2$ at $r/a = 0.75$.

(2) The spectra of probe current J^+ were always broad and roughly invariant in the frequency range 10 kHz – 1 MHz. Below 100 kHz the spectra were typically flat, and above 100 kHz the spectral power fell like $\bar{f}^{\alpha}$ where $\alpha = 2$–3. The only coherent activity was that associated with strong MHD before disruption.

(3) A stable edge regime was found in the cold low-current plasma obtained when the neutral H_2 filling pressure was unusually high. Relative fluctuation levels below 3% were present in these very short-lived discharges.

(4) The edge turbulence was observed to be independent of the presence or absence of an outer limiter in the chamber.

(5) The edge turbulence was approximately unchanged over a range of local edge collisionality $\nu_{ei}/\nu_{Te} \cong 0.1$–$10$. Thus the local collisionality did not seem to be the controlling factor in determining the local edge turbulence.

(6) The level of turbulence did seem to vary with the parameter ρ_s/L_n which measures the strength of the radial density gradient. However, this scaling came mainly from the observed decrease in fluctuation level with increased density toward the plasma centre and not from observed variations in ρ_s or dn/dx.

Two subjects which were not mentioned in the present paper but which are important in understanding the edge plasma are: (i) the spatial structure of the turbulence, and (ii) the correlation between the density turbulence and other fluctuating variables, such as potential, magnetic field or possibly temperature. Particularly interesting is the relationship between density fluctuations and radial particle transport [7, 19, 27], an understanding of which may be relevant for the interior regions of the tokamak as well.

ACKNOWLEDGEMENTS

The authors wish to thank Dr. P.C. Liewer for many discussions of the theory and many suggestions which

were incorporated in this work. Also, the authors would like to acknowledge helpful discussions with all of the theorists whose work is cited in Section 4.4. Finally, the authors thank F. Cosso for expert help in constructing the computer interfacing.

REFERENCES

[1] MAZZUCATO, E., Phys. Rev. Lett. **48** (1982) 1828.
[2] SLUSHER, R.E., SURKO, C.M., Phys. Fluids **23** (1980) 2438.
[3] SAITO, T., HAMADA, Y., YAMASHITA, T., IKEDA, M., NAKAMURA, M., TANAKA, S., Nucl. Fusion **21** (1981) 1005.
[4] SEMET, A., MASE, A., PEEBLES, W.A., LUHMANN, N.C., ZWEBEN, S., Phys. Rev. Lett. **45** (1980) 445.
[5] EQUIPE TFR, in Plasma Physics and Controlled Nuclear Fusion Research 1980 (Proc. 8th Int. Conf. Brussels, 1980) Vol.1, IAEA, Vienna (1981) 425.
[6] ZWEBEN, S.J., TAYLOR, R.J., Nucl. Fusion **21** (1981) 193.
[7] ZWEBEN, S.J., LIEWER, P.C., GOULD, R.W., in Plasma Surface Interactions (Proc. 5th Int. Conf. Gatlinburg, 1982); J. Nucl. Mater. **111/112** (1982) 39.
[8] OHTSUKA, H., KIMURA, H., SHIMOMURA, S., MAEDA, H., YAMAMOTO, S., NAGAMI, M., UEDA, N., KITSUNEZAKI, A., NAGASHIMA, T., Plasma Phys. **20** (1978) 749.
[9] PROUDFOOT, G., HARBOUR, P.J., J. Nucl. Mater. **93/94** (1980) 413.
[10] GOODALL, D.H.J., J. Nucl. Mater. **111/112** (1982) 11.
[11] ZWEBEN, S.J., McCHESNEY, J., GOULD, R.W., Nucl. Fusion **23** (1983) 825.
[12] SURKO, C.M., SLUSHER, R.E., Waves and turbulence in tokamak fusion plasmas, Science **221** 4613 (1983) 817.
[13] TANG, W.M., Nucl. Fusion **18** (1978) 1089.
[14] HORTON, W., Drift Wave Turbulence and Anomalous Transport, Univ. Texas Rep. IFSR-35 (1981).
[15] LIEWER, P.C., Measurements of microscopic fluctuations in tokamaks and comparison with theories of anomalous transport – a review (in preparation for Nucl. Fusion).
[16] CHEN, F.F., in Plasma Diagnostic Techniques, Academic Press, New York (1975) 113.
[17] SANMARTIN, J.R., Phys. Fluids **13** (1970) 103.
[18] STAIB, P., J. Nucl. Mater. **111/112** (1982) 109.
[19] ZWEBEN, S.J., TAYLOR, R.J., Nucl. Fusion **23** (1983) 513.
[20] LAFRAMBOISE, J.G., RUBINSTEIN, J., Phys. Fluids **19** (1976) 1900.
[21] PARROT, M.J.M., STOREY, L.R.O., PARKER, L.W., LAFRAMBOISE, J.G., Phys. Fluids **25** (1982) 2388.
[22] PARK, H., YU, C.X., PEEBLES, W.A., LUHMANN, N.C., SAVAGE, R., Rev. Sci. Instrum. **53** (1982) 1535.
[23] LUHMANN, N.C., Jr., PEEBLES, W.A., BROWER, D., YU, C.X., JUNGWIRTH, D., SAVAGE, R., "Multichannel FIR scattering observations on TEXT", in Plasma Science (Proc. IEEE Conf. San Diego, 1983) (1983) paper 5A8.
[24] STRACHAN, J.D., BRETZ, N., MAZZUCATO, E., BARNES, C.W., BOYD, D., COHEN, S.A., HOVEY, J., KAITA, R., MEDLEY, S.S., SCHMIDT, G., TAIT, G., VOSS, D., Nucl. Fusion **22** (1982) 1145.
[25] ZWEBEN, S.J., LIEWER, P.C., GOULD, R.W., Phys. Fluids (1983).
[26] HORTON, W., Bull. Am. Phys. Soc. **27**, 8, Part II, paper RW1 (Oct. 1982).
[27] LEVINSON, S.J., BEALL, J.M., POWERS, E.J., BENGSTON, R.D., Space-Time Statistics of the Turbulence in a Tokamak Edge Plasma, Texas Univ., Austin, Fusion Research Center, Rep. FRCR-259 (Oct. 1983).
[28] WOOTTON, A.J., private communication, 1983.
[29] HASEGAWA, A., WAKATANI, M., Phys. Rev. Lett. **50** (1983) 682.
[30] TERRY, P., DIAMOND, P.H., The Spectrum of Dissipative Drift-Wave Turbulence in a Tokamak Edge Plasma, Texas Univ., Austin, Inst. for Fusion Studies, Rep. IFS-114 (Nov. 1983).
[31] TERRY, P.W., HORTON, W., Phys. Fluids **26** (1983) 106.
[32] WALTZ, R.E., DOMINGUEZ, R.R., Drift Wave Turbulence with Wave-Wave and Wave-Particle Nonlinear Effects in a Sheared Slab, General Atomic Co., San Diego, CA, Tech. Rep. GA-A16946 (1983).
[33] MEISS, J.D., HORTON, W., Phys. Fluids **25** (1982) 1838.
[34] FREIDBERG, J.P., MOLVIG, K., BEASLEY, C.O., Jr., VAN RIJ, W., in Plasma Physics and Controlled Nuclear Fusion Research 1982 (Proc. 9th Int. Conf. Baltimore, 1982) Vol.1, IAEA, Vienna (1983) 249.
[35] DIAMOND, P.H., SIMILON, P.L., TERRY, P.W., HORTON, C.W., MAHAJAN, S.M., et al., in Plasma Physics and Controlled Nuclear Fusion Research 1982 (Proc. 9th Int. Conf. Baltimore, 1982) Vol.1, IAEA, Vienna (1983) 259.
[36] CALLEN, J.D., CARRERAS, B.A., DIAMOND, P.H., BENCHIKH-LEHOCINE, M.E., GARCIA, L., HICKS, H.R., in Plasma Physics and Controlled Nuclear Fusion Research 1982 (Proc. 9th Int. Conf. Baltimore, 1982) Vol.1, IAEA, Vienna (1983) 297.
[37] CARRERAS, B.A., GAFFNEY, P.W., HICKS, H.R., CALLEN, J.D., Phys. Fluids **25** (1982) 1231.
[38] HASSAM, A.B., DRAKE, J.F., Phys. Fluids **26** (1983) 133.
[39] MOTLEY, R.W., Nucl. Fusion **21** (1981) 1541.
[40] STANGEBY, P.C., Nucl. Fusion **22** (1982) 1383.
[41] EL-NADI, A., HASSAN, H., Phys. Fluids **25** (1982) 2140.
[42] WAGNER, F., BECKER, G., BEHRINGER, K., CAMPBELL, D., EBERHAGEN, A., et al., Phys. Rev. Lett. **50** (1982) 1408.

(Manuscript received 25 July 1983
Final manuscript received 24 November 1983)